


Identification of Early Response to Anti-Angiogenic Therapy in Recurrent Glioblastoma: Amide Proton Transfer–weighted and Perfusion-weighted MRI compared with Diffusion-weighted MRI

Ji Eun Park, MD, PhD • Ho Sung Kim, MD, PhD • Seo Young Park, PhD • Seung Chai Jung, MD, PhD • Jeong Hoon Kim, MD, PhD • Hye-Young Heo, PhD

From the Department of Radiology and Research Institute of Radiology (J.E.P., H.S.K., S.C.J.), Department of Clinical Epidemiology and Biostatistics (S.Y.P.), and Department of Neurosurgery (J.H.K.), University of Ulsan College of Medicine, Asan Medical Center, 43 Olympic-ro 88, Songpa-Gu, Seoul 05505, Korea; and Department of Radiology, Johns Hopkins University, Baltimore, Md (H.Y.H.). Received June 18, 2019; revision requested July 16, 2019; revision received December 24; accepted December 30. **Address correspondence to** H.S.K. (e-mail: radhskim@gmail.com).

Supported by a National Research Foundation of Korea (NRF) grant funded by the Korean government (MSIP) (grants NRF-2017R1A2A2A05001217 and NRF-2017R1C1B2007258).

Conflicts of interest are listed at the end of this article.

Radiology 2020; 00:1–10 • <https://doi.org/10.1148/radiol.2020191376> • Content codes: 

Background: Amide proton transfer (APT) MRI has the potential to demonstrate antitumor effects by reflecting biologically active tumor portion, providing different information from diffusion-weighted imaging (DWI) or dynamic susceptibility contrast (DSC) imaging.

Purpose: To evaluate whether a change in APT signal intensity after antiangiogenic treatment is predictive of early treatment response in recurrent glioblastoma.

Materials and Methods: In this retrospective study, APT MRI, DWI, and DSC imaging were performed in patients with recurrent glioblastoma from July 2015 to April 2019, both before treatment and 4–6 weeks after initiation of bevacizumab (follow-up). Progression was based on pathologic confirmation or clinical-radiologic assessment, and progression patterns were defined as local enhancing or diffuse nonenhancing. Changes in mean and histogram parameters (fifth and 95th percentiles) of APT signal intensity, apparent diffusion coefficient, and normalized cerebral blood volume (CBV) between imaging time points were calculated. Predictors of 12-month progression and progression-free survival (PFS) were determined by using logistic regression and Cox proportional hazard modeling and according to progression type.

Results: A total of 54 patients were included (median age, 56 years [interquartile range, 49–64 years]; 24 men). Mean APT signal intensity change after bevacizumab treatment indicated a low 12-month progression rate (odds ratio [OR], 0.36; 95% confidence interval [CI]: 0.13, 0.90; $P = .04$) and longer PFS (hazard ratio: 0.38; 95% CI: 0.20, 0.74; $P = .004$). High mean normalized CBV at follow-up was associated with a high 12-month progression rate (OR, 20; 95% CI: 2.7, 32; $P = .04$) and shorter PFS (hazard ratio, 9.4; 95% CI: 2.3, 38; $P = .002$). Mean APT signal intensity change was a significant predictor of diffuse nonenhancing progression (OR, 0.27; 95% CI: 0.06, 0.85; $P = .047$), whereas follow-up 95th percentile of the normalized CBV was a predictor of local enhancing progression (OR, 7.1; 95% CI: 2.4, 15; $P = .04$).

Conclusion: Early reduction in mean amide proton transfer signal intensity at 4–6 weeks after initiation of antiangiogenic treatment was predictive of a better response at 12 months and longer progression-free survival in patients with recurrent glioblastoma, especially in those with diffuse nonenhancing progression.

©RSNA, 2020

Online supplemental material is available for this article.

Glioblastoma is typically characterized by marked angiogenesis mediated by vascular endothelial growth factor, and there has therefore been much interest in treatment focused on targeting this protein. Although antiangiogenic agents that target vascular endothelial growth factor signaling (eg, bevacizumab) have been increasingly used in recurrent glioblastoma, the precise quantification of radiologic response to antiangiogenic treatment is challenging because of the treatment's unique effects on the tumor vasculature (1,2). Specifically, reduced contrast material enhancement on conventional contrast material–enhanced MRI scans may not necessarily correspond to a reduction in viable tumor after antiangiogenic treatment. Although

the Response Assessment in Neuro-Oncology criteria (3) were specifically designed to better assess radiologic response in patients with glioma treated with antiangiogenic agents, they are not sufficient for early prediction of response because they require late confirmatory scans to rule out pseudoresponse. Therefore, the development of novel and reliable imaging biomarkers for assessing the response to antiangiogenic treatment addresses a major unmet clinical need to improve disease management.

Clinical studies of patients with recurrent glioblastoma have shown that diffusion-weighted imaging (DWI) is helpful for stratifying patients before bevacizumab treatment, with a low apparent diffusion coefficient (ADC)

Abbreviations

ADC = apparent diffusion coefficient, APT = amide proton transfer, CBV = cerebral blood volume, CI = confidence interval, DSC = dynamic susceptibility contrast, DWI = diffusion-weighted imaging, FLAIR = fluid-attenuated inversion recovery, OR = odds ratio, PFS = progression-free survival, ROI = region of interest

Summary

Early reduction of amide proton transfer signal intensity at MRI 4–6 weeks after initiation of bevacizumab treatment from baseline imaging was associated with a favorable 12-month outcome in recurrent glioblastoma and was superior to the apparent diffusion coefficient.

Key Results

- Early reduction in mean amide proton transfer (APT) signal intensity 4–6 weeks after initiation of bevacizumab treatment indicated lower odds of 12-month progression (odds ratio [OR], 0.36; $P = .04$) and was associated with long progression-free survival (hazard ratio, 0.38; $P = .004$).
- According to the progression pattern, the mean APT signal intensity change (OR, 0.27; $P = .047$) was a predictor of a diffuse nonenhancing type of progression.

being associated with shorter progression-free survival (PFS) (4–6). The main advantage of using DWI with ADC is its ability to enable assessment of viable tumor cellularity, a feature considered independent of the status of tumor-related angiogenesis and vascularity. However, posttreatment ADC decreases include not only cell death, but also decreased Brownian motion due to reduced permeability, chronic hypoxia, and coagulative necrosis (6–8). An association between cerebral blood volume (CBV) reduction and longer survival has been shown (9,10), but this may be limited because recurrence after antiangiogenic treatment is not caused solely by neo-angiogenesis, but also by vascular co-option with nonenhancing recurrence (8).

Amide proton transfer (APT) MRI depicts the exchangeable amide protons in the backbone of mobile proteins (11,12) and has been shown to demonstrate the active tumor portion that has high cellularity and proliferation at histopathologic correlation (13). We speculated that antitumor effect measured with APT MRI may be more specific for tumor physiologic features and less confounded by changes in tumor vascularity and permeability. The hypothesis of this study was that early changes in parameters obtained with APT MRI are different from those obtained with DWI and perfusion-weighted imaging and could be helpful in stratifying patient response for antiangiogenic therapy. The purpose of this study was therefore to evaluate whether a change in the APT MRI signal intensity after antiangiogenic treatment is predictive of early treatment response in recurrent glioblastoma. We further explored whether early changes in imaging biomarkers differed according to progression patterns and compared with DWI and perfusion-weighted imaging.

Materials and Methods

Patients

This retrospective data evaluation was approved by the institutional review board of Asan Medical Center (approval number:

2019–0473), and the requirement to obtain informed patient consent was waived. The study lasted from July 26, 2015, to April 1, 2019. Patients were retrospectively selected from the neuro-oncology databases of Asan Medical Center. Inclusion criteria for recurrent glioblastoma were as follows: (a) patients had histologically confirmed glioblastoma with progression diagnosed on the basis of clinical data and MRI after standard treatment consisting of surgery, concurrent chemotherapy and radiation therapy (hereafter, chemoradiotherapy), and adjuvant temozolomide; (b) patients were more than 3 months from chemoradiotherapy, to avoid the confounding factor of radiation necrosis (pseudoprogression); (c) patients were not subject to therapies other than antiangiogenic treatment, including repeat surgery, repeat irradiation, or immunotherapies, because of the patient's clinical status and indication; and (d) availability of pretreatment (before bevacizumab treatment) and first follow-up images from MRI with DWI, dynamic susceptibility contrast (DSC) imaging, and APT MRI after bevacizumab treatment. Of 156 potentially eligible patients, 70 patients who did not undergo two consecutive DWI, DSC, or APT MRI acquisitions; 23 patients who were within 3 months from chemoradiotherapy; and six patients whose treatment was confounded by gamma knife radiosurgery or immunotherapy at the same time as bevacizumab treatment were excluded.

At the time of progression, imaging patterns were determined according to whether the increased enhancement or high fluid-attenuated inversion recovery (FLAIR) signal intensity change included the primary site. This criterion was adopted from previous studies in which the radiologic patterns were described as local, diffuse, distant, and/or multifocal progression (14–16). Because these reports did not include quantitative imaging parameters, modification for application to region of interest (ROI)-based imaging analysis was deemed necessary. The three main patterns of progression recorded were (a) local enhancing progression (focus of contrast enhancement at or within 3 cm of the primary site), (b) diffuse nonenhancing progression (local contrast-enhancing tumor remains stable, but an area of abnormal FLAIR hyperintensity is not concordant and extends more than 3 cm from the primary site), and (c) distant progression (new focus of contrast enhancement or area of abnormal FLAIR hyperintensity extending more than 3 cm from the primary site with intervening normal-appearing white matter). The progression pattern was classified by two neuroradiologists (J.E.P. and H.S.K., with 5 and 20 years of experience in neuro-oncologic imaging, respectively) in consensus, on the basis of the imaging findings at the time of progression. Patients with distant-type progression ($n = 3$) were further excluded because this was mainly caused by multifocal gliomagenesis. Figure E1 (online) demonstrates cases of local enhancing and diffuse nonenhancing progression types.

A total of 54 consecutive patients met the aforementioned criteria and were enrolled. All patients experienced a first recurrence after standard treatment. The included patients (a) received regular treatment every week with bevacizumab (Avastin; Roche, Welwyn Garden City, England; 10 mg per kilogram body weight) for tumor progression; (b) had undergone pretreatment DWI and APT MRI; (c) had undergone first follow-up DWI

and APT MRI within 6 weeks after bevacizumab treatment; and (d) were available for follow-up MRI for up to 12 months.

Response Assessment, PFS, and Progression Pattern

Patients were assessed with MRI at 2–3-month intervals. A diagnosis of tumor progression at 6 months was based on pathologic confirmation following second-look surgery or clinical-radiologic assessment. Clinical-radiologic diagnosis was conducted by an experienced neuroradiologist (H.S.K.) and a neurosurgeon (J.H.K., with 30 years of experience in neuro-oncology practice), who reviewed the imaging data and medical records to establish a diagnosis by using the Response Assessment in Neuro-Oncology criteria (3). An objective response was defined as a complete or partial response at two consecutive MRI examinations with reduced or stable doses of corticosteroids.

PFS was defined as the time from antiangiogenic treatment until death (ascertained by means of an institutional linkage to the national health care system) or the first imaging report indicating worsening or progression. Patients were censored at the date of medical record abstraction or at the date of last imaging report, whichever came first.

Twelve-month progression after bevacizumab treatment and PFS from initiation of bevacizumab therapy, until disease progression or death, were analyzed.

Image Acquisition and Processing

The brain tumor imaging protocol was performed with a 3-T unit (Ingenia 3.0 CX; Philips Healthcare, Best, the Netherlands) and included conventional and advanced sequences, including T2-weighted, T2-weighted FLAIR, and precontrast and postcontrast T1-weighted images. Parameters for conventional MRI are described in Appendix E1 (online). Advanced imaging included DWI, APT-weighted imaging before injection of contrast material, and DSC imaging after injection of contrast material. Parameters for DWI included repetition time msec/echo time msec, 3000/56; diffusion gradient encoding, $b = 0$ and 1000 sec/mm²; field of view, 250 × 250 mm; matrix, 256 × 256; slice thickness, 5 mm; and gap, 2 mm. ADC images were calculated from the DWI images obtained with b values of 1000 and 0 sec/mm². The parameters for DSC MRI were as follows: 1808/40; flip angle, 35°; field of view, 240 × 240 mm; slice thickness, 5 mm; gap, 2 mm; and matrix, 128 × 128. The total acquisition time for DSC MRI was 1 minute 54 seconds.

APT-weighted images were acquired with a three-dimensional turbo spin-echo sequence by applying an off-resonance radiofrequency pulse with an overall duration of 2 seconds (50 msec × 40 elements) and amplitude of 2 μT. The acquisition parameters were as follows: 5000/6; field of view, 250 × 250 mm; matrix, 224 × 224; and slice thickness, 5 mm. The z-axis coverage was 75 mm with 15 slices, with an imaging time of 7 minutes 5 seconds. The centric elliptical k-space ordering scheme was used, which enabled rapid three-dimensional image acquisition (17). The APT signal intensity was calculated on the MRI console from the magnetization transfer ratio (magnetization transfer ratio = $1 - S_{\text{sat}}/S_0$, where S_{sat} and S_0 are the image signal intensities measured with and without radiofrequency saturation, respectively) asymmetry analysis reflecting water signal changes

(11). APT maps (defined as APT = magnetization transfer ratio [+3.5 ppm] – magnetization transfer ratio [–3.5 ppm]) were calculated on the MRI console based on the δB0 point-by-point corrected interpolated images.

Data from two consecutive brain tumor imaging sessions were chosen: the examination performed before bevacizumab treatment (pretreatment) and the examination performed at the first follow-up after bevacizumab treatment and at least 4 weeks apart from the pretreatment examination (initial response). The last-visit MRI used either the brain tumor imaging protocol (including conventional and advanced sequences) or conventional imaging parameters. Advanced sequences were not available for all patients because either the patient's clinical status did not allow long-duration follow-up imaging or the patient underwent imaging with routine conventional sequences.

Quantitative Analysis

Imaging data were transferred to an independent workstation and processed with software (nordicICE, version 4.0.6 [NordicNeuroLab, Bergen, Norway] and Matlab, version R2017b [MathWorks, Natick, Mass]). The whole-brain relative CBV was calculated from the DSC images by using numeric integration of the time-concentration curve after correcting for leakage of contrast material. Leakage correction was performed by using the Weisskoff-Boxerman method (18). We then normalized the relative CBV images with the mean signal intensity of the contralateral normal-appearing centrum semiovale (diameter of ROI, 4 mm), which was manually selected by a researcher with 2 years of experience in neuroimaging processing. FLAIR, ADC, normalized CBV, and APT maps were coregistered to the anatomic and FLAIR images, which acted as a reference. An experienced neuroradiologist (J.E.P.), who was blinded to the clinical data and any other imaging data except the FLAIR images, drew ROIs over the areas with a high signal intensity on each slice of the FLAIR images. The ROI was carefully checked to ensure it included active tumor tissue but excluded cystic, necrotic, or hemorrhagic areas and APT-weighted signal intensity that was falsely increased (19) owing to mobile proteins and peptides.

The average ADC, normalized CBV, and APT were calculated for the entire ROI. Cumulative ADC, normalized CBV, and APT histogram parameters were generated for the entire segmented volume of interest by using a bin size of 100. After removal of the highest and lowest values beyond 3 standard deviations, the fifth percentile of the ADC and the 95th percentile of the APT and normal CBV were calculated, with these being considered to be representative of the lowest and highest robust values, respectively (20).

Changes in the ADC, normalized CBV, APT-weighted parameters, and volume of the FLAIR high-signal-intensity volume of interest were analyzed. Changes in within-patient mean ADC, normalized CBV, and APT-weighted parameters; fifth percentile of the ADC and 95th percentile of the normalized CBV and the APT; and FLAIR volume of interest between pretreatment imaging and imaging performed at the first follow-up were further calculated by subtracting the value at baseline

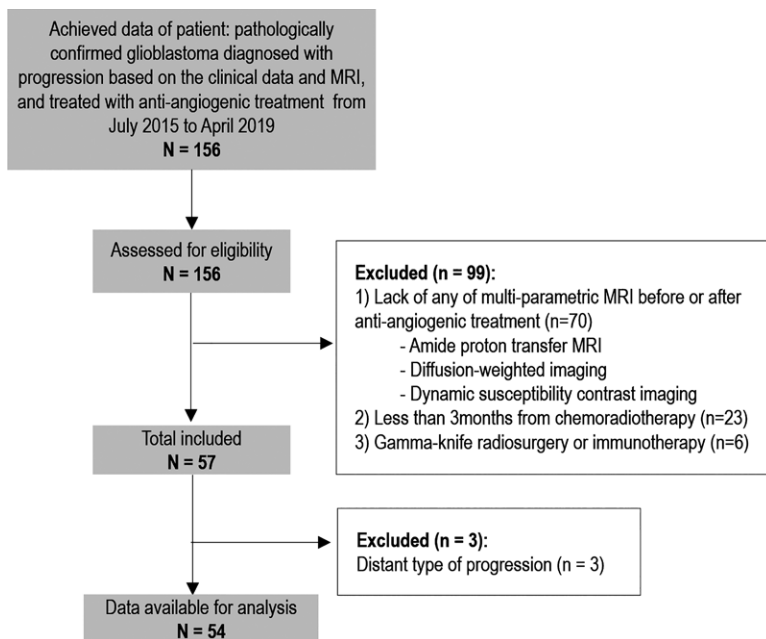


Figure 1: Flowchart shows inclusion and exclusion process of our study.

imaging from the value at first follow-up; these results were included in the analysis.

Reproducibility of APT Measurements

To ensure the stability of the APT signal intensity across the longitudinal analysis, circular ROIs of a uniform 7-mm diameter were drawn on the APT images in the opposite-side normal-appearing white matter by a neuroradiologist (S.C.J., with 8 years of experience in neuroradiology). These ROIs were drawn on the corona radiata to avoid leukoaraiosis or dilated perivascular space, and the mean APT values were calculated for the pretreatment and first follow-up acquisitions.

Statistical Analysis

All described results are reported as medians with ranges or 95% confidence intervals (CIs) for continuous variables and as frequencies or percentages for categorical variables. All imaging parameters were checked for normality by using the D'Agostino-Pearson test. All parameters were normally distributed. The longitudinal reproducibility of APT measurements was evaluated by calculating the intraclass correlation coefficient with a two-way random effects model. Paired *t* tests were used to determine the significance of changes in imaging parameters between the first follow-up and pretreatment examinations. Student *t* tests were used to determine differences between the 12-month progression and nonprogression groups.

The primary purpose of this study was to determine whether APT MRI has predictive value for antiangiogenic treatment. With use of mean ADC, normalized CBV, APT, and change in mean signal intensity value, a multivariable logistic regression model was constructed to find significant pretreatment and first follow-up imaging parameters for predicting progression at 12 months, in addition to changes between baseline and first follow-up examinations. A Cox proportional hazard regression

model was used to explore the relationship between overall PFS and the imaging parameters.

Because there was no known imaging biomarker found to be associated with the pattern of progression, we further conducted an exploratory analysis to find imaging biomarkers by using the mean signal intensity value and the histogram parameters (fifth percentile of the ADC, 95th percentile of the APT and normalized CBV) according to the pattern of progression. Both logistic regression and Cox proportional hazard regression models were applied separately to patients with local enhancing progression and diffuse nonenhancing progression. Receiver operating characteristic curve analysis was performed for each imaging parameter to determine the optimal cutoff point for predicting 12-month progression. The areas under the receiver operating characteristic curve were calculated.

Isocitrate dehydrogenase 1 and 2 mutation status was further tested for association with PFS. For significant imaging parameters in the Cox proportional hazard model, the optimal cutoff for the predictor was estimated by using the maxstat (21)

function in R statistical software (R, version 3.4.3; R Foundation for Statistical Computing, Vienna, Austria), with $P < .05$ considered to indicate a statistically significant difference.

Results

Patients, Bevacizumab Regimen, and Responses

A flowchart for the inclusion process is shown in Figure 1. The patient demographics, bevacizumab regimens, and responses are summarized in Table 1. Thirty women and 24 men were enrolled, with a median age of 56 years at initial diagnosis. All patients were treated with concurrent chemoradiotherapy and six cycles of adjuvant temozolomide. The median time from concurrent chemoradiotherapy to diagnosis of recurrence was 10 months (range, 6–35 months). The patients were classified as having recurrence for the first time ($n = 37$), second time ($n = 14$), or third time ($n = 3$). Pretreatment images were obtained at a median of 10 days (range, 0–30 days) before treatment. The first follow-up images were obtained 4–6 weeks after the first bevacizumab treatment (median, 36 days; range, 27–57 days).

Bevacizumab was continued either as monotherapy ($n = 42$) or in combination with other chemotherapies with irinotecan ($n = 1$) or temozolomide ($n = 11$). There was no significant difference in the treatment regimen between the progression and nonprogression groups ($P = .16$). The median number of bevacizumab cycles was nine (range, 4–24 cycles), with most patients (42 of 54 [78%]) receiving bevacizumab monotherapy. The median follow-up period after bevacizumab treatment was 12.7 months (range, 2.6–37.6 months). Until the time of censoring (August 20, 2019), 43 of the 54 patients (80%) had developed disease progression or had died, whereas 11 (20%) were alive without disease progression. Through 12 months, 38 patients showed progression, which was confirmed with pathologic

Table 1: Baseline Patient Demographics, Bevacizumab Regimens, and Responses

Parameter	Value
Clinical data	
Median age (y)	56 (49–64)
Sex	
M	24
F	30
Median Karnofsky performance status score at recurrence	80 (70–90)
Isocitrate dehydrogenase mutation status	
Wild	49
Mutant	5
MGMT promoter methylation status	
Methylated	15
Unmethylated	21
Not available	18
Extent of resection at pretreatment surgery	
Biopsy	7
Partial or subtotal resection	19
Gross total resection	28
Recurrence	
First	37
Second	14
Third	3
Median time from chemoradiation therapy to diagnosis of recurrence (mo)	10 (6–35)
Bevacizumab regimen	
Bevacizumab alone	42
Bevacizumab plus chemotherapy	12
Median no. of bevacizumab cycles	9 (6–20)
Agent started with bevacizumab	
Temozolomide	11
Irinotecan	1
Response	
Median follow-up period after bevacizumab treatment (mo)	12.7 (5.6–33.8)
No. of patients with disease progression at last visit*	43 (80)
Median progression-free survival (mo)	8.3 (5.0–30.1)
Progression pattern	
Local enhancing	20
Diffuse nonenhancing	23

Note.—Unless otherwise specified, data are numbers of patients ($n = 54$) and numbers in parentheses are the interquartile range. MGMT = oxygen 6-methylguanine-DNA methyltransferase.

* Number in parentheses is the percentage.

examination in five patients and with clinical-radiologic assessment in 33. The mean APT signal intensity (\pm standard deviation) in the normal-appearing white matter was $0.31\% \pm 0.27$ on pretreatment images and $0.29\% \pm 0.25$ on the first follow-up images. The intraclass correlation coefficient for APT signal intensity between the pretreatment and first follow-up images was 0.86 (95% CI: 0.81, 0.94).

Prediction of 12-month Progression and PFS

The imaging parameters from pretreatment and first follow-up examinations are summarized in Table E1 (online). ADC and APT values decreased significantly from pretreatment to first follow-up (all $P < .001$ with paired t test), whereas normalized CBV values did not show a significant change ($P > .05$). There was no statistically significant difference in mean APT

or ADC values or tumor volume between the 12-month progression and nonprogression groups at either pretreatment imaging or first follow-up imaging, although mean normalized CBV values were higher at first follow-up in the progression group ($P = .04$).

Multivariable logistic regression analysis was performed to identify MRI parameters for stratifying 12-month progression (Table 2). Mean APT change significantly stratified patients according to 12-month progression ($P = .04$); a large decrease in mean APT (mean APT change: odds ratio [OR], 0.36; 95% CI: 0.13, 0.90) indicated lower odds for 12-month progression. High posttreatment mean normalized CBV (OR, 20; 95% CI: 2.7, 32; $P = .04$) was associated with a higher probability of 12-month progression.

In the Cox proportional hazard modeling, only mean APT change was a significant predictor of PFS, with a large decrease in mean APT being associated with long PFS (mean APT change: hazard ratio, 0.38; 95% CI: 0.20, 0.74; $P = .004$). High posttreatment mean APT (OR, 1.8; 95% CI: 1.1, 3.1; $P = .02$) and normalized CBV (OR, 9.4; 95% CI: 2.3, 38; $P = .002$) were associated with short PFS. The optimal cutoff for mean APT change for stratifying longer- and shorter-PFS groups was 0.073. Figure 2 shows the Kaplan-Meier survival curves and risk

table based on the mean APT change. No definite association was found between isocitrate dehydrogenase 1 and 2 mutation status and PFS.

Differences in Imaging Parameters according to Type of Progression

Table E2 (online) shows the differences in imaging parameters according to the type of progression. Both ADC and APT values decreased significantly in patients with no progression, local enhancing progression, and diffuse nonenhancing progression.

We further explored whether the imaging parameters could help predict the different types of progression, especially prediction of local enhancing progression and diffuse nonenhancing progression. The significant results of this analysis are summarized in Table 3, and the complete results are shown in Table

Table 2: Imaging Parameters for Stratifying 12-month Progression and Progression-free Survival in Patients Treated with Bevacizumab

Imaging Parameter	12-month Progression			Progression-free Survival		
	Odds Ratio	95% CI	P Value	Hazard Ratio	95% CI	P Value
Before treatment						
Mean ADC ($\times 10^{-3}$ mm ² /sec)	1.0	1.0, 1.0	.55	1.0	0.9, 1.0	.10
Mean APT-weighted signal intensity (%)	0.7	0.4, 1.4	.36	1.0	0.6, 1.7	.96
Mean nCBV	10	0.6, 20	.16	9.8	0.8, 39	.12
FLAIR volume (mL)	1.0	1.0, 1.0	.18	1.0	1.0, 1.0	.42
First follow-up						
Mean ADC ($\times 10^{-3}$ mm ² /sec)	1.0	0.9, 1.0	.38	1.0	0.9, 1.0	.06
Mean APT-weighted signal intensity (%)	1.4	0.7, 3.2	.38	1.8	1.1, 3.1	.02
Mean nCBV	20	2.7, 32	.04	9.4	2.3, 38	.002
FLAIR volume (mL)	1.0	1.0, 1.0	.67	1.0	1.0, 1.0	.75
Change between pretreatment and first follow-up imaging						
Mean ADC ($\times 10^{-3}$ mm ² /sec)	1.0	1.0, 1.0	.90	1.0	1.0, 1.0	.95
Mean APT-weighted signal intensity (%)	0.4	0.1, 1.0	.04	0.4	0.2, 0.7	.004
Mean nCBV	0.3	0.0, 1.8	.23	0.6	0.1, 3.0	.49
FLAIR volume (mL)	1.0	1.0, 1.0	.20	1.0	1.0, 1.0	.46

Note.—Stratification was performed by using multivariate logistic regression and Cox hazard analysis. Odds and hazard ratios indicate relative change in odds and hazard incurred by each imaging parameter per 1-unit increase, respectively. ADC = apparent diffusion coefficient, APT = amide proton transfer, CI = confidence interval, FLAIR = fluid-attenuated inversion recovery, nCBV = normalized relative cerebral blood volume.

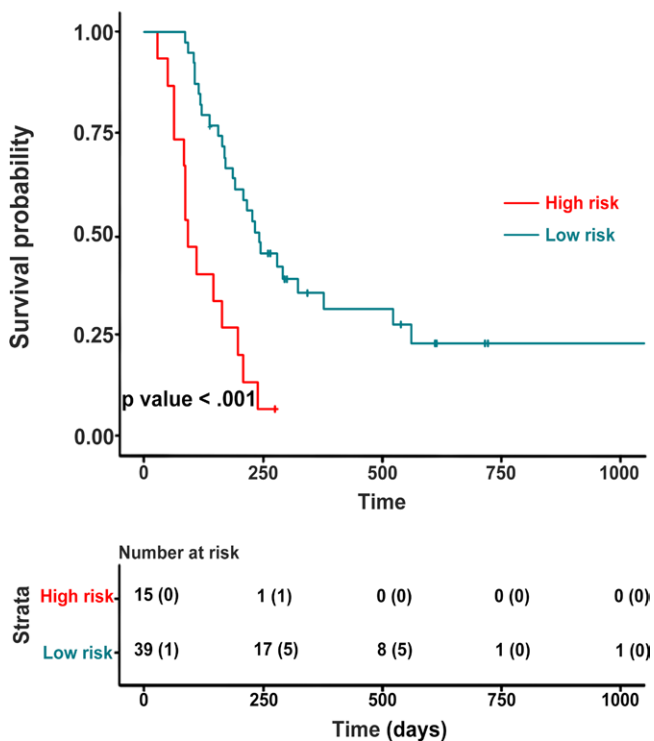


Figure 2: Graph shows Kaplan-Meier estimates of progression-free survival (PFS) based on change in mean amide proton transfer (APT)-weighted signal intensity before and after bevacizumab treatment. Cohort is stratified into shorter (high risk) and longer (low risk) PFS groups based on cut-off value of 0.073 mean APT-weighted signal intensity change. Numbers in parentheses are numbers of censored data.

E3 (online). According to logistic regression, high posttreatment 95th percentile of the normalized CBV (OR, 7.14; 95% CI: 2.40, 15.05; $P = .04$) was a significant predictor of local enhancing progression, with an area under the receiver operating characteristic curve of 0.78 (95% CI: 0.62, 0.94); low mean APT change (OR, 0.27; 95% CI: 0.06, 0.85; $P = .047$) was a significant predictor of diffuse nonenhancing progression, with an area under the receiver operating characteristic curve of 0.70 (95% CI: 0.52, 0.88). Figure 3 shows images from conventional MRI, APT MRI, DSC imaging, and DWI of example cases of nonprogression, local enhancing progression, and diffuse nonenhancing progression.

Discussion

Early imaging biomarkers of tumor response, especially those reflecting an antiangioma effect, may correlate with survival and may be useful in customizing antiangiogenic therapy in patients with recurrent glioblastoma. In this study, we examined early changes in diffusion-weighted, perfusion-weighted, and amide proton transfer (APT) MRI findings between pretreatment and follow-up imaging performed within 6 weeks of commencing bevacizumab treatment and evaluated their usefulness in predicting progression and identifying response in patients with recurrent glioblastoma. The results demonstrated that a large decrease in the mean APT signal intensity between pretreatment imaging and 4–6-week follow-up imaging indicated early effective treatment until 12 months (odds ratio [OR], 0.36; $P = .04$) and may predict longer progression-free survival (PFS) (hazard ratio = 0.38; $P = .004$). Interestingly, the imaging parameters showed different predictive values ac-

Table 3: Imaging Parameters Associated with Progression in Patients with Bevacizumab-treated Recurrent Glioma

Imaging Parameter	Enhancing Progression (<i>n</i> = 20) vs No Progression (<i>n</i> = 7)					Nonenhancing Progression (<i>n</i> = 23) vs No Progression (<i>n</i> = 7)				
	OR	95% CI	<i>P</i> Value	AUC	95% CI	OR	95% CI	<i>P</i> Value	AUC	95% CI
nCBV 95th percentile at first follow-up	7.1	2.4, 15	.04	0.78	0.62, 0.94	3.1	0.93, 7.5	.20
Mean change in APT between pretreatment and first follow-up	0.6	0.2, 2.0	.46	0.3	0.1, 0.9	.047	0.70	0.52, 0.88

Note.—ORs indicate relative change in odds incurred by each imaging parameter per 1-unit increase. APT = amide proton transfer-weighted signal intensity, AUC = area under the receiver operating characteristic curve, CI = confidence interval, nCBV = normalized relative cerebral blood volume, OR = odds ratio.

according to the pattern of progression. A smaller decrease in the mean APT signal intensity was more predictive of diffuse nonenhancing progression (OR, 0.27; *P* = .047), whereas a high normalized cerebral blood volume (CBV) at initial follow-up after antiangiogenic treatment may be predictive of future local enhancing progression (95th percentile of normalized CBV: OR, 7.1; *P* = .04).

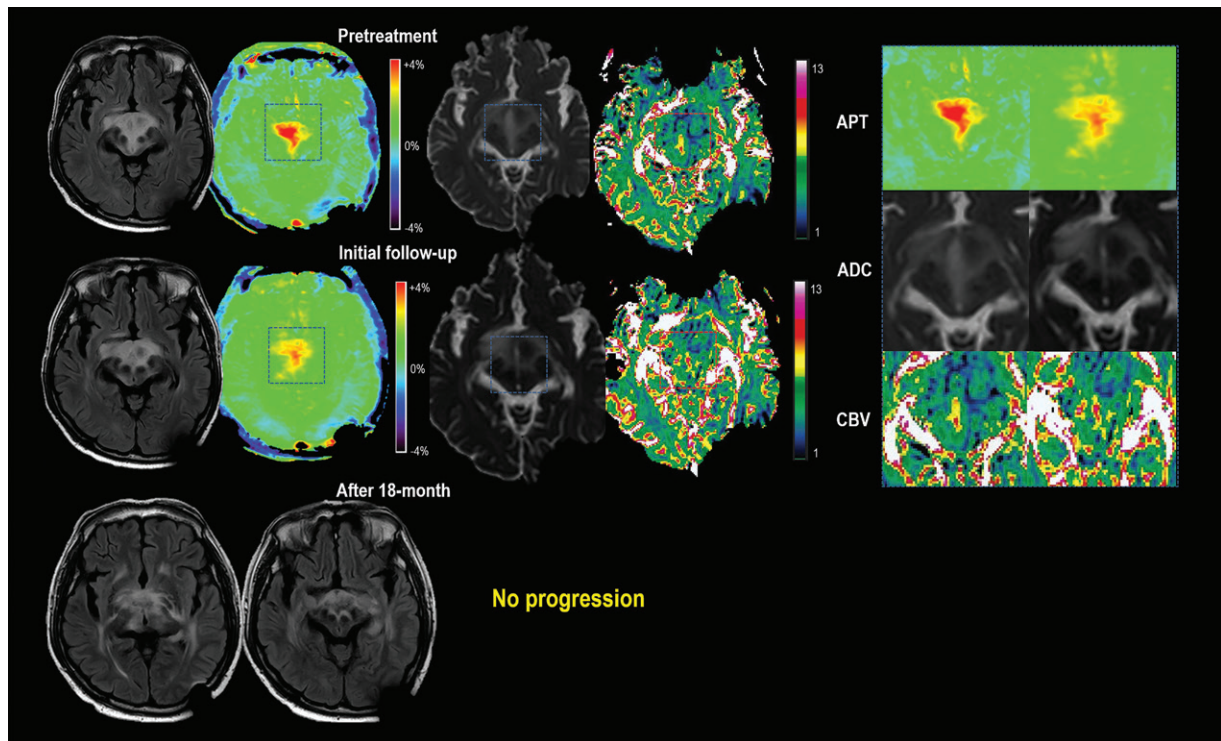
Decreasing CBV after bevacizumab treatment has been shown to be a predictor of overall survival in recurrent glioblastoma (9,10). Our results were similar; posttreatment high normalized CBV was associated with a high probability of 12-month progression. On the other hand, vascular normalization has been documented as occurring as early as 1–14 days after antiangiogenic treatment (22), and this can act as a confounding factor on the response assessment with Brownian motion-based diffusion-weighted MRI. In general, reduced permeability decreases ADCs, and a previous longitudinal study in patients with recurrent glioblastoma showed that ADC decreased in all lesions except one after 2 weeks of bevacizumab treatment (23). Moreover, low ADC in bevacizumab-treated tissue included tissue damage from coagulative necrosis (7,23). This complex mechanism limits the usefulness of ADC for predicting treatment response after bevacizumab therapy, even though high ADC before bevacizumab treatment is correlated with elongation of PFS and overall survival (4–6,23).

After antiangiogenic treatment, an antitumor effect has been shown (24); a decrease in choline-to-creatinine ratio occurs between days 28 and 56, a period similar to the period of 4–6 weeks after treatment that was used for follow-up imaging in our study. The APT signal intensity has also been shown to be moderately correlated with the choline-to-creatinine ratio at imaging (25), and a recent imaging-guided stereotactic biopsy study in post-treatment gliomas demonstrated that high APT signal intensity correlated with the proliferation index of Ki-67 (26), allowing determination of the active tumor region. This supports that the decrease in APT signal intensity is a direct indication of a decrease in active tumor proliferation. We found that an antitumor effect at the initial follow-up indicated stability in 12-month progression and was predictive of PFS in recurrent glioblastoma. APT MRI has been used to demonstrate the antitumor effects of radiation (27) and chemoradiation therapies (28) in patients with glioblastoma, but to our knowledge this is the first longitudinal study to show such effects after antiangiogenic treatment.

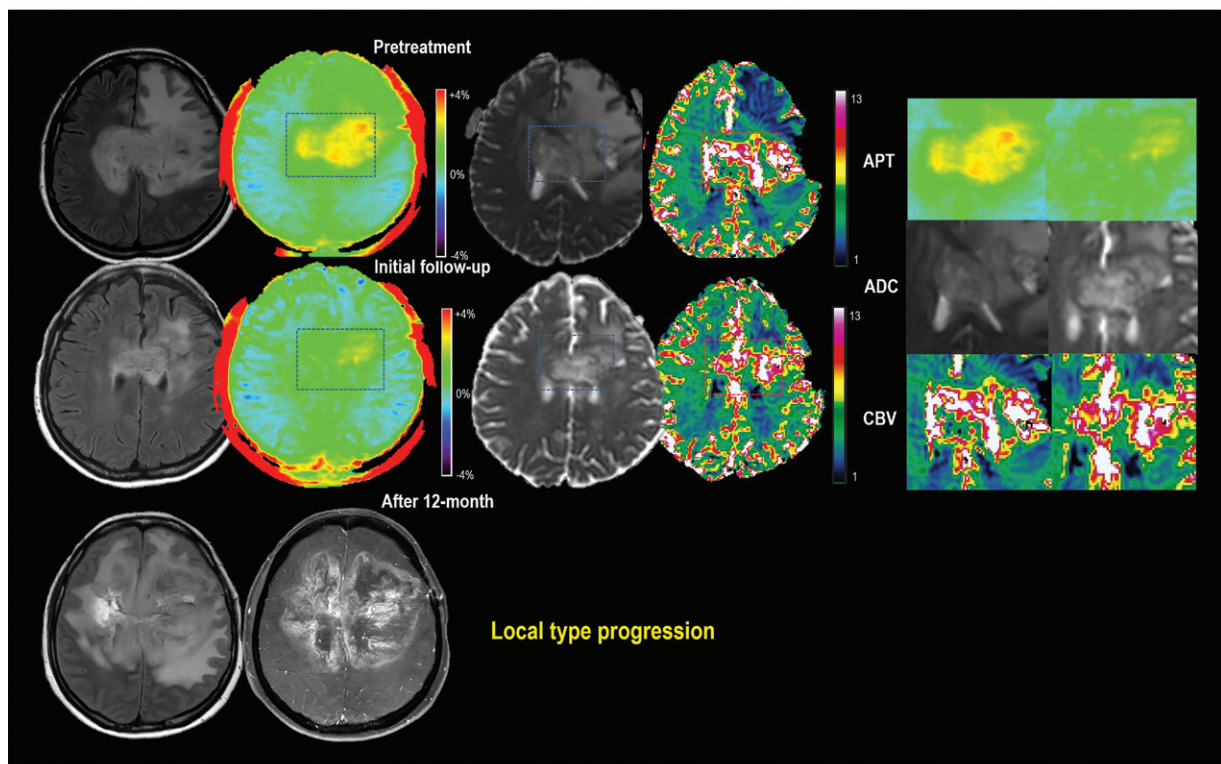
The radiologic patterns of treatment failure have been categorized into local, distant, diffuse, and multifocal patterns of

progression by using standard-of-care imaging (14,15). Local progression, which includes the initial ROI, indicates failure of local disease control and is different from diffuse progression, which is promoted by continuous blockage of vascular proliferation and tumor escape through vascular co-option, with change to a more invasive pathologic phenotype (29). One study found the results to be heterogeneous, with the pattern of progression having no impact on PFS and overall survival (15); another proposed that the diffuse subtype demonstrates longer survival (14). The aforementioned patterns are subject to the limitation that they are based on FLAIR image hyperintensity; it may be difficult to differentiate edema from tumor on FLAIR images, and no study to our knowledge has combined their use with quantitative imaging parameters. In our study, a large decrease in the APT signal intensity was indicative of low probability of diffuse nonenhancing progression, and low normalized CBV at follow-up was indicative of low probability of local enhancing progression. Our exploratory study incorporated the concept of both a radiologic pattern of treatment failure and physiologic information from APT and normalized CBV, which may be helpful for guiding imaging biomarker-based studies.

The limitations of this study included the limited number of patients, the retrospective nature of the study, and the overlap between patients with and patients without progression. This can be more problematic in a cross-sectional design study, but we used longitudinal analysis and demonstrated change over time within individuals to examine cause-and-effect relationships, especially before and 4–6 weeks after antiangiogenic treatment. We believe that future prospective studies are needed to confirm the relationship between APT reduction and antitumor activity. Second, overall survival was not assessed, because more than 20% of patients were censored at the time of study, and the treatment regimens applied after progression following bevacizumab treatment included gamma knife radiosurgery and immunotherapy. Third, another important issue is the possible contribution of tumor pH to APT signal intensity, because the exchange rate of amide protons is catalyzed with a base within a physiologic pH range (11). Interestingly, in a previous study in which phosphorus 31 MR spectroscopy was used (30), recurrent glioblastoma following antiangiogenic treatment showed increased intracellular pH at progression (pH: 7.08 ± 0.035) compared with baseline (pH: 7.06 ± 0.032) at 3-T imaging. However, the slight change in pH (0.02 pH unit) may be negligible at APT MRI (corresponding to about 0.12%) (11). In contrast to

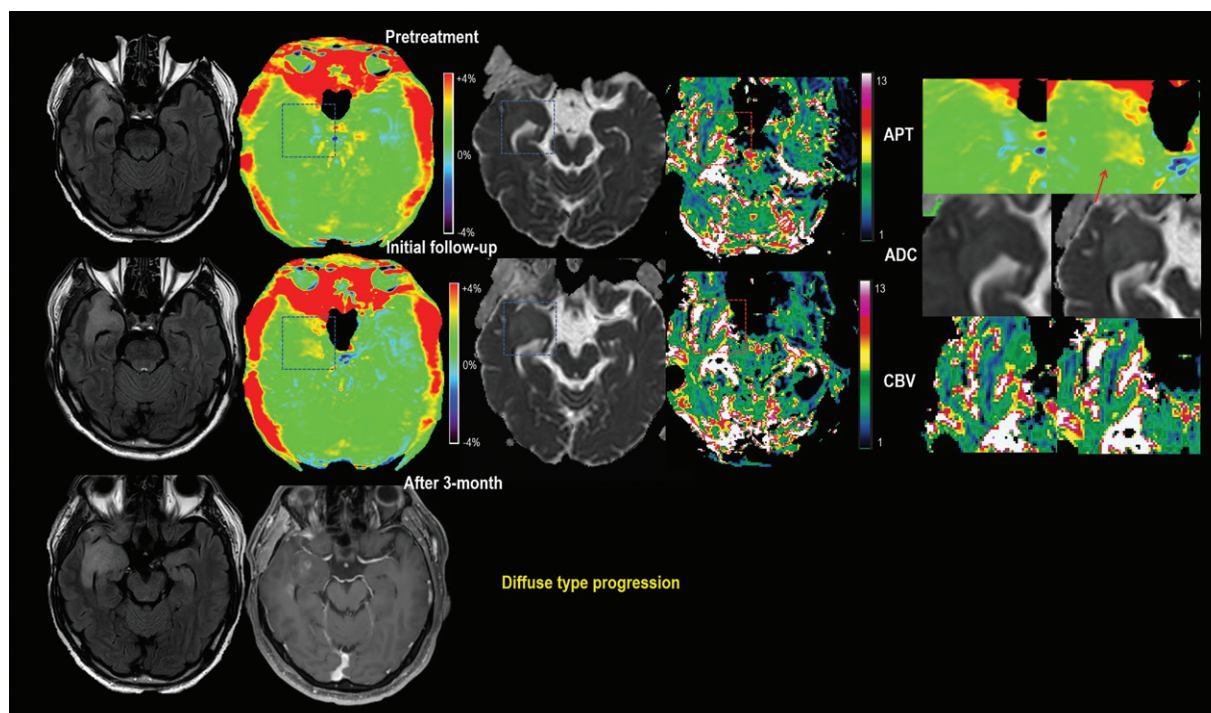


a.



b.

Figure 3: Longitudinal apparent diffusion coefficient (ADC), normalized relative cerebral blood volume (CBV), and amide proton transfer (APT) images from T2-weighted fluid-attenuated inversion recovery MRI performed before and after bevacizumab treatment. **(a)** No progression. Images in 45-year-old man show decrease in both APT and ADC at initial follow-up. Posttreatment normalized CBV is low. Last follow-up images obtained 18 months after treatment reveal no signs of progression. **(b)** Local contrast-enhancing progression. Images in 55-year-old woman show large decrease in APT in central portion of the tumor, with decrease in ADC also demonstrated at periphery. Posttreatment normalized CBV remained high. Images at 12 months show contrast-enhancing progression (Fig 3 continues).



c.

Figure 3 (continued). (c) Diffuse nonenhancing progression. Images in 58-year-old man show slight increase in APT, with decrease in ADC also demonstrated in central portion of the tumor. Posttreatment normalized CBV is low. Images at 3 months show diffuse nonenhancing type progression.

the progression group, the APT signal intensity declined from pretreatment to initial follow-up imaging in the nonprogression group at 12 months, a finding that was presumably related to fewer cytosolic mobile proteins due to lower cellularity and disrupted cytoplasm (31,32), but further study is required to investigate the source of the signal. Finally, the radiologist who drew the ROI was later involved in judging the progression patterns. Although the evaluator was blinded to any other images other than those obtained with the conventional MRI sequence and to clinical data at the time of the ROI drawing, complete independence of evaluators involved in image analysis from outcome measures is more desirable.

In conclusion, we observed that large decreases in amide proton transfer (APT) MRI signal intensity 4–6 weeks after initiation of bevacizumab treatment were associated with a better response at 12 months and longer progression-free survival in patients with recurrent glioblastoma. Decreases in the APT signal intensity were predictive of diffuse nonenhancing progression, whereas high normalized cerebral blood volume at follow-up was predictive of local enhancing progression. The prediction of progression after antiangiogenic treatment merits further investigation with prospectively designed imaging biomarker studies.

Author contributions: Guarantor of integrity of entire study, H.S.K.; study concepts/study design or data acquisition or data analysis/interpretation, all authors; manuscript drafting or manuscript revision for important intellectual content, all authors; approval of final version of submitted manuscript, all authors; agrees to ensure any questions related to the work are appropriately resolved, all authors; literature research, J.E.P., H.S.K., H.Y.H.; clinical studies, J.E.P., H.S.K., S.C.J., J.H.K.; experimental studies, J.E.P., H.Y.H.; statistical analysis, J.E.P., H.S.K., S.Y.P.; and manuscript editing, J.E.P., H.S.K., H.Y.H.

Disclosures of Conflicts of Interest: J.E.P. disclosed no relevant relationships. H.S.K. disclosed no relevant relationships. S.Y.P. disclosed no relevant relationships. S.C.J. disclosed no relevant relationships. J.H.K. disclosed no relevant relationships. H.Y.H. disclosed no relevant relationships.

References

- Jain RK. Antiangiogenesis strategies revisited: from starving tumors to alleviating hypoxia. *Cancer Cell* 2014;26(5):605–622.
- Sitohy B, Nagy JA, Dvorak HF. Anti-VEGF/VEGFR therapy for cancer: reassessing the target. *Cancer Res* 2012;72(8):1909–1914.
- Wen PY, Macdonald DR, Reardon DA, et al. Updated response assessment criteria for high-grade gliomas: response assessment in neuro-oncology working group. *J Clin Oncol* 2010;28(11):1963–1972.
- Pope WB, Kim HJ, Huo J, et al. Recurrent glioblastoma multiforme: ADC histogram analysis predicts response to bevacizumab treatment. *Radiology* 2009;252(1):182–189.
- Ellingson BM, Gerstner ER, Smits M, et al. Diffusion MRI Phenotypes Predict Overall Survival Benefit from Anti-VEGF Monotherapy in Recurrent Glioblastoma: Converging Evidence from Phase II Trials. *Clin Cancer Res* 2017;23(19):5745–5756.
- Rahman R, Hamdan A, Zweifler R, et al. Histogram analysis of apparent diffusion coefficient within enhancing and nonenhancing tumor volumes in recurrent glioblastoma patients treated with bevacizumab. *J Neurooncol* 2014;119(1):149–158.
- Nguyen HS, Milbach N, Hurrell SL, et al. Progressing Bevacizumab-Induced Diffusion Restriction Is Associated with Coagulative Necrosis Surrounded by Viable Tumor and Decreased Overall Survival in Patients with Recurrent Glioblastoma. *AJNR Am J Neuroradiol* 2016;37(12):2201–2208.
- Thomas A, Rosenblum M, Karimi S, DeAngelis LM, Omuro A, Kaley TJ. Radiographic patterns of recurrence and pathologic correlation in malignant gliomas treated with bevacizumab. *CNS Oncol* 2018;7(1):7–13.
- Schminda KM, Prah M, Connelly J, et al. Dynamic-susceptibility contrast agent MRI measures of relative cerebral blood volume predict response to bevacizumab in recurrent high-grade glioma. *Neuro Oncol* 2014;16(6):880–888.
- Schminda KM, Zhang Z, Prah M, et al. Dynamic susceptibility contrast MRI measures of relative cerebral blood volume as a prognostic marker for overall survival in recurrent glioblastoma: results from the ACRIN 6677/RTOG 0625 multicenter trial. *Neuro Oncol* 2015;17(8):1148–1156.
- Zhou J, Payen J-F, Wilson DA, Traystman RJ, van Zijl PCM. Using the amide proton signals of intracellular proteins and peptides to detect pH effects in MRI. *Nat Med* 2003;9(8):1085–1090.
- Zhou J, Heo HY, Knutsson L, van Zijl PCM, Jiang S. APT-weighted MRI: Techniques, current neuro applications, and challenging issues. *J Magn Reson Imaging* 2019;50(2):347–364.
- Togao O, Yoshiura T, Keupp J, et al. Amide proton transfer imaging of adult diffuse gliomas: correlation with histopathological grades. *Neuro Oncol* 2014;16(3):441–448.

14. Nowosielski M, Wiestler B, Goebel G, et al. Progression types after antiangiogenic therapy are related to outcome in recurrent glioblastoma. *Neurology* 2014;82(19):1684–1692.
15. Pope WB, Xia Q, Paton VE, et al. Patterns of progression in patients with recurrent glioblastoma treated with bevacizumab. *Neurology* 2011;76(5):432–437.
16. Shapiro LQ, Beal K, Goenka A, et al. Patterns of failure after concurrent bevacizumab and hypofractionated stereotactic radiation therapy for recurrent high-grade glioma. *Int J Radiat Oncol Biol Phys* 2013;85(3):636–642.
17. Heo HY, Xu X, Jiang S, et al. Prospective acceleration of parallel RF transmission-based 3D chemical exchange saturation transfer imaging with compressed sensing. *Magn Reson Med* 2019;82(5):1812–1821.
18. Boxerman JL, Schmainda KM, Weisskoff RM. Relative cerebral blood volume maps corrected for contrast agent extravasation significantly correlate with glioma tumor grade, whereas uncorrected maps do not. *AJNR Am J Neuroradiol* 2006;27(4):859–867.
19. Park JE, Kim HS, Park KJ, Choi CG, Kim SJ. Histogram Analysis of Amide Proton Transfer Imaging to Identify Contrast-enhancing Low-Grade Brain Tumor That Mimics High-Grade Tumor: Increased Accuracy of MR Perfusion. *Radiology* 2015;277(1):151–161.
20. Chung WJ, Kim HS, Kim N, Choi CG, Kim SJ. Recurrent glioblastoma: optimum area under the curve method derived from dynamic contrast-enhanced T1-weighted perfusion MR imaging. *Radiology* 2013;269(2):561–568.
21. Wright MN, Dankowski T, Ziegler A. Unbiased split variable selection for random survival forests using maximally selected rank statistics. *Stat Med* 2017;36(8):1272–1284.
22. Pope WB, Lai A, Nghiemphu P, Mischel P, Cloughesy TF. MRI in patients with high-grade gliomas treated with bevacizumab and chemotherapy. *Neurology* 2006;66(8):1258–1260.
23. Nagane M, Kobayashi K, Tanaka M, et al. Predictive significance of mean apparent diffusion coefficient value for responsiveness of temozolomide-refractory malignant glioma to bevacizumab: preliminary report. *Int J Clin Oncol* 2014;19(1):16–23.
24. Kim H, Catana C, Ratai EM, et al. Serial magnetic resonance spectroscopy reveals a direct metabolic effect of cediranib in glioblastoma. *Cancer Res* 2011;71(11):3745–3752.
25. Park JE, Kim HS, Park KJ, Kim SJ, Kim JH, Smith SA. Pre- and Posttreatment Glioma: Comparison of Amide Proton Transfer Imaging with MR Spectroscopy for Biomarkers of Tumor Proliferation. *Radiology* 2016;278(2):514–523.
26. Jiang S, Eberhart CG, Lim M, et al. Identifying recurrent malignant glioma after treatment using amide proton transfer-weighted MR imaging: A validation study with image-guided stereotactic biopsy. *Clin Cancer Res* 2019;25(2):552–561.
27. Desmond KL, Mehrabian H, Chavez S, et al. Chemical exchange saturation transfer for predicting response to stereotactic radiosurgery in human brain metastasis. *Magn Reson Med* 2017;78(3):1110–1120.
28. Park KJ, Kim HS, Park JE, Shim WH, Kim SJ, Smith SA. Added value of amide proton transfer imaging to conventional and perfusion MR imaging for evaluating the treatment response of newly diagnosed glioblastoma. *Eur Radiol* 2016;26(12):4390–4403.
29. de Groot JF, Fuller G, Kumar AJ, et al. Tumor invasion after treatment of glioblastoma with bevacizumab: radiographic and pathologic correlation in humans and mice. *Neuro Oncol* 2010;12(3):233–242.
30. Wenger KJ, Hattungen E, Franz K, Steinbach JP, Bähr O, Pilatus U. Intracellular pH measured by ³¹P-MR-spectroscopy might predict site of progression in recurrent glioblastoma under antiangiogenic therapy. *J Magn Reson Imaging* 2017;46(4):1200–1208.
31. Zhang P, Guo Z, Zhang Y, et al. A preliminary quantitative proteomic analysis of glioblastoma pseudoprogression. *Proteome Sci* 2015;13(1):12.
32. Yan K, Fu Z, Yang C, et al. Assessing Amide Proton Transfer (APT) MRI Contrast Origins in 9 L Gliosarcoma in the Rat Brain Using Proteomic Analysis. *Mol Imaging Biol* 2015;17(4):479–487.